

High temperature mechanical behavior of $\text{Al}_2\text{O}_3\text{--MgO--C}$ refractories for steelmaking use[☆]

Leonardo Musante^a, Vanesa Muñoz^b, Marcelo H. Labadie^c, Analía G. Tomba Martinez^{b,*}

^aTenaris Siderca R&D Campana (2804), Buenos Aires, Argentina

^bLaboratorio de Materiales Estructurales – División Cerámicos - INTEMA CONICET – Facultad de Ingeniería/UNMdP, Mar del Plata (7600), Buenos Aires, Argentina

^cGerencia de Materiales y Tecnología – Ternium Siderar Centro Siderúrgico Gral. Savio San Nicolás (2009), Buenos Aires, Argentina

Received 9 September 2010; received in revised form 22 October 2010; accepted 10 December 2010

Available online 3 March 2011

Abstract

The advantages of $\text{Al}_2\text{O}_3\text{--MgO--C}$ (AMC) refractories are achieved mainly by the incorporation of graphite and the formation of spinel by solid reaction between alumina and magnesia. Regarding other members of oxide-C refractories (such as MgO-C bricks) and others properties (such as the slag corrosion resistance or the PLC), the information about the mechanical behavior of this type of refractories is scarce. In this work, the mechanical behavior of commercial AMC brick used in steelmaking ladles was studied by stress-strain curves in compression at RT and 1000 °C (nitrogen atmosphere). Before the mechanical testing, a comprehensive characterization of AMC materials was performed by several techniques: XRD, DTA/TGA, SEM/EDS, aggregate size distribution analysis and densities, porosities and thermal expansion measurements. Mechanical parameters such as fracture strength and strain, yield stress and Young modulus were determined together with the main characteristics of the fracture. In order to study the transformations occurred during the stay at high temperature, the specimens tested at 1000 °C were analyzed by the same techniques used for the as-received bricks characterization (with the exception of the thermal expansion analysis). The AMC refractories displayed differences in the mechanical behavior and its dependence on the testing temperature. These results were explained considering the differences in the composition and microstructure of both refractories and in their thermal transformations.

© 2011 Elsevier Ltd and Techna Group S.r.l. All rights reserved.

Keywords: $\text{Al}_2\text{O}_3\text{--MgO--C}$ refractories; High temperature; Stress-strain curves

1. Introduction

In spite of the increment in the bauxite price that restricts the use of $\text{Al}_2\text{O}_3\text{--MgO--C}$ (AMC) bricks in steelmaking plants (working lining of ladles and furnaces) these refractories maintain their high consumption level due to their excellent properties. Beside the advantages associated to the presence of carbon commonly in the form of graphite flakes, i.e., the increment in thermal conductivity, thermal shock resistance and slag attack resistance, the formation of spinel (MgAl_2O_4) by reaction between periclase and alumina induces an expansion in the operative thermal conditions that helps to

counterbalance the wear of the brick join [1–9]. This reaction also produces microcracking because the thermal expansion difference between the spinel and the periclase and the alumina (in a lower degree) which favors the toughness of the refractory (although it could also lead to slag penetration, so an optimum content of MgO is required) [1,5,9]. The spinel itself is used extensively as refractory due to its high melting point and high slag corrosion resistance.

The superior mechanical properties of carbon based refractories is related to the inelastic deformation (or flexibility) given by the graphite. This behavior enables the brick to accommodate the applied stress through ‘yield’, increasing the strain to fracture. From this point of view, the fracture strain in addition to the fracture stress is therefore a desirable data and cannot be obtain in a conventional mechanical test (MOR, CCS, HMOR). The structure flexibility is a very important property that determines the durability of refractory materials in steel work and represents a substantial criterion for the durability of

[☆] SIDERAR S.A.I.C provided the financial support for the conduct of the research under SIDERAR S.A.I.C.-CONICET agreement (RD No. 2286/05).

* Corresponding author. Tel.: +54 223 4816600; fax: +54 223 4810046.

E-mail address: agtomba@fi.mdp.edu.ar (A.G. Tomba Martinez).

refractory lining. Stress–strain curves are a suitable tool to obtain this information [10]; actually, several parameters such as fracture strength, fracture strain, yield stress and Young modulus may be obtained in a unique test, with the additional advantage of using variable conditions of temperature and atmosphere. Moreover, constitutive equation of materials can be obtained from stress–strain curves, which is essential nowadays for structural calculus of vessels by finite element codes. Together with the analysis of deformation and fracture mechanisms, stress–strain relationships are useful to improve the material design.

Despite of their excellent properties, during materials service life, severe conditions such as thermal gradients, mechanical loading by stirring or charge impact, abrasion due to the presence of gases, particles and liquids in movement, can degrade AMC refractories. For this reason, and with the aim of evaluating the performance in service and establishing material design criteria, the knowledge of the mechanical behavior at high temperature is indispensable. Conversely to other members of the oxide-C family for which there are a large amount of information, as in the case of MgO–C bricks, or regarding other properties of AMC materials such as slag corrosion resistance or PLC, there is few data of high temperature mechanical behavior of AMC refractories. The use of stress–strain curves for the mechanical evaluation of this sort of materials is even more unusual.

The general objective of this work is to evaluate the mechanical behavior of commercial AMC bricks used in steelmaking ladles at temperatures near to those in-service. In a first stage, stress–strain curves were performed at room temperature and at 1000 °C, a temperature close to that used in the pre-heating of the ladles. A comprehensive characterization of both commercial refractories was performed including: mineralogical (XRD and SEM/EDS), thermal (DTA/TGA), microstructural (optical and scanning electron microscopies) and thermal expansion analyses and densities and porosities measurements. The mechanical testing was conducted in controlled atmosphere and several techniques (similar to those employed for as-received materials) were used after the tests in view of identifying the main factors determining the mechanical response. With this aim, the differences in the mechanical behavior and mechanical parameters were analyzed in function of the compositional and microstructural characteristics of the materials and their changes during the tests at high temperature.

2. Experimental

2.1. Materials

Two AMC commercial bricks fabricated by the same manufacturer (Argentina) and labelled AM1 and AM2, were studied. Both refractories have resin as organic binder and are employed in steelmaking ladles. AM1 brick is used in the wall and the less loaded regions of the bottom and AM2 is employed in the impact zone of the ladle bottom.

The bricks were characterized by several techniques. The mineralogical analysis was carried out by X-ray diffraction

(XRD; Philips PW3710) on powdered samples (<mesh 70), using Cu K α radiation at 40 kV and 30 mA, with Ni filter. The Rietveld method was employed for quantitative analysis (FullProf software). The bulk density (ρ_b) and the apparent porosity (π_a) were determined based on DIN EN 993-1 (DIN 51056) standard [11]. The pycnometric density (ρ_{pic}) was measured on powdered samples (<mesh 70) employing kerosene in accordance with an internal method based on the ASTM C329- 88 standard [12]. The true porosity (π_t) and the close porosity (π_c) were obtained by calculation using the following relationships: $\pi_t = (1 - \rho_b/\rho_{pic}) \times 100$ and $\pi_c = \pi_t - \pi_a$. The thermal expansion under load (0.6 MPa) was determined in N $_2$ up to 1000 °C (Instron 8501) on cylindrical specimens (50 mm in diameter, 50 mm in height). The linear change was measured using contact extensometry (scissor extensometer with alumina knives). The thermal differential (DTA; Shimadzu DTA-50) and thermogravimetric (TGA; Shimadzu TGA-50) analyses were performed on powdered samples (<mesh 70) up to 1200 °C (10 °C/min) in air. The microstructure of bricks was observed by optical microscopy up to 150 \times (binocular glass Zeiss) and scanning electron microscopy (SEM; Philips XL30) coupled with elementary analysis using an X-ray energy dispersion spectroscopy (EDS) detecting unit. The surfaces for observation were obtained by transversal cut of cylinders previously stuffed in resin to avoid the crumbling of the specimen, and polishing with SiC papers (320 grit) using kerosene as lubricant/coolant. The digital image analysis was performed using the software Corel Photo-Paint to enhance the digital quality of the images and Image Pro Plus 9.0 to measure the size of MgO and Al $_2$ O $_3$ particles (≥ 0.06 mm).

2.2. Mechanical tests

Stress–strain curves were determined under uniaxial compressive pressure using a universal servohydraulic testing machine (Instron 8501) with a high stiffness framework and high density mullite/alumina push-rods (60 mm in diameter). The compressive load was applied parallel to the cylinder axis and alumina disks were placed between the testing specimens and the push-rods. The mechanical tests were carried out at room temperature (RT) and 1000 °C (heating rate of 5 °C/min), using an electrical furnace (SFL) with Mo $_2$ Si heating elements. During the high temperature mechanical tests, a continuous flow of nitrogen gas was employed to generate a non-oxidant atmosphere.

The testing specimens (cylinders of 27 mm in diameter and 40 mm in height) were obtained by cutting and machining (70 grit) with diamond tools; the cylinder axis was parallel to the direction of the main compressive loading on the bricks in service. The change in the specimen height (from which the deformation was calculated) was measured by contact extensometry using a capacitive extensometer (± 0.6 μ m; 25 mm of gauge length) with SiC knives suitable for high temperature measurements. The tests were carried out in displacement (of the actuator) control with a constant rate of 0.1 mm/min, up to the specimen failure.

The mechanical behavior characteristic of each material was analyzed from the stress–strain curves and the following mechanical parameters were determined: Young's modulus (E), yield stress (σ_Y), mechanical strength (σ_R), and fracture strain (ε_R). The Young's modulus was determined as the slope of the linear portion of the stress–strain curve. The value of σ_Y was considered as the stress where the curve deviates from linearity in 1%; this parameter is not commonly analyzed in the literature for this sort of materials. The ratio σ_Y/σ_R (in percentage) was considered as a measure of the deviation from the linear elastic behavior by inelasticity (due to a softening by microcracking, for example) or plasticity (due to viscous flow, for instance); thus, this parameter was also related to the type of dominant mechanical behavior (ductile or brittle). In regard to the mechanical strength, it was taken as the maximum stress displayed in the stress–strain curve that is a common criterion used in this type of materials. The strain corresponding to this condition was taken as ε_R .

The way in which the specimens failed at the end of the test was evaluated considering the following typical fractures: (a) 'ductile', with low noise, notable previous strain and several cracks; (b) 'brittle', with high noise, small previous strain and a unique crack; (c) 'quasi-brittle', with intermediate characteristics. Moreover, the main fracture paths were also analyzed by visual inspection.

The microstructural changes occurred in the materials during the high temperature mechanical tests were evaluated using several techniques: mineralogical analysis by XRD, DTA/TGA, density and porosity measurements, and observation by optical microscopy and SEM/EDS. The same methodologies used for as-received materials were employed. These data are complementary to the information obtained from the mechanical testing and make possible to analyse the main factors determining the mechanical behavior and the deformation and fracture mechanisms.

3. Results

3.1. Materials characterization

In both refractories, AM1 and AM2, α - Al_2O_3 as corundum, together with MgO as periclase and C as graphite were

identified as the main crystalline phases by XRD (Table 1). The amount of Al_2O_3 was in excess in respect to spinel (less than 20 wt.% of MgO) in both AMC materials. Moreover, the weight percentage and mol ratios between MgO and Al_2O_3 contents were similar in both refractories: 9–10 and 4.0–4.4, respectively. In the material AM1, peaks of mullite ($3\text{Al}_2\text{O}_3 \cdot 2\text{SiO}_2$), rutile (TiO_2) and tialite (Al_2TiO_5) were also identified; the phases' contents were around 10 wt.%, 1 wt.% and 3 wt.%, respectively. In both AMC refractories, low intensity peaks were assigned to metals, aluminium (AM1: ≈ 1 wt.% and AM2: ≈ 2 wt.%) and silicon (AM1 and AM2: ≈ 1 wt.%), added as antioxidant.

Aggregates of sinter and electrofused grains were identified in the microstructural observation of the refractories. The global aggregates size as well as the size of Al_2O_3 and MgO particles (≥ 0.06 mm) aggregates were larger for AM1 refractory (Table 1). The mean size of alumina aggregates was larger than that of periclase for both types of materials. In Fig. 1, SEM images of the matrix of AM1 and AM2 are shown. Calcined bauxite aggregates (characterized by the presence of an intergranular glassy phase) and tabular alumina (without glassy phase between grains) aggregates in a minor amount, were identified in AM1. Mullite, rutile and tialite detected by XRD came from bauxite aggregates. The presence of these secondary phases could be the reason of the lower content of Al_2O_3 pointed out by XRD in AM1. Sinter aggregates of MgO were also detected. Graphite flakes and antioxidants as Al were clearly observed in the bonding phase (Fig. 1b) while the presence of silicon cannot be confirmed by SEM/EDS. On the other hand, AM2 only exhibited aggregates of brown alumina (characterized by a smooth texture and the presence of intergranular glassy phase). As in AM1, graphite flakes, sinter MgO aggregates and Al antioxidants particles (< 50 μm) were also distinguished (Fig. 1d). The bonding phase of AM1 exhibited higher porosity than that of AM2.

The values of densities and porosities of AMC refractories are reported in Table 1. The higher pycnometric density of AM2 were partially attributed to the contribution of a larger amount of alumina, with higher density than magnesia (3980 kg/m^3 with respect to 3580 kg/m^3) and the absence of secondary phases as mullite (3180 kg/m^3). AM1 has a higher volume

Table 1
Characterization of as-received refractory materials.

| | | AM1 | AM2 |
|---------------|--|-----------------|-----------------|
| wt.% (XRD) | Al_2O_3 | 67 \pm 5 | 80 \pm 5 |
| | MgO | 6 \pm 5 | 8 \pm 5 |
| | C | 11 \pm 5 | 9 \pm 5 |
| | ρ_{pic} (kg/m^3) | 3630 \pm 30 | 3710 \pm 60 |
| | ρ_{b} (kg/m^3) | 3010 \pm 10 | 3280 \pm 10 |
| | π_{a} (%) | 8 \pm 1 | 7 \pm 1 |
| | π_{t} (%) | 17 \pm 1 | 11 \pm 1 |
| | π_{c} (%) | 9 \pm 1 | 4 \pm 1 |
| | DTA | 440 °C | 895 °C |
| | Δm (TGA) | −2.2 wt.% | −3.7 wt.% |
| D_{50} (mm) | global | 1.12 \pm 0.02 | 0.76 \pm 0.02 |
| | Al_2O_3 | 1.15 \pm 0.02 | 0.80 \pm 0.02 |
| | MgO | 1.04 \pm 0.02 | 0.69 \pm 0.02 |
| | | 440 °C | 855 °C |
| | | −3.0 wt.% | −5.4 wt.% |

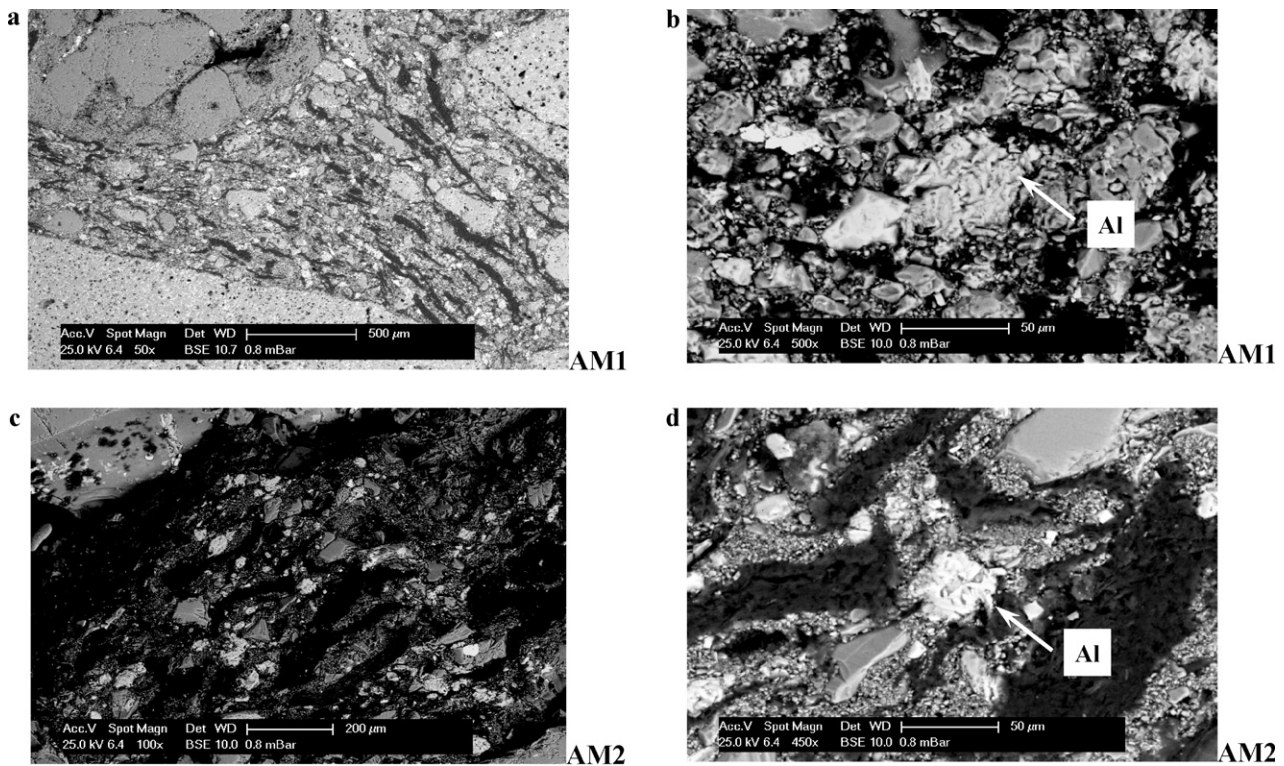


Fig. 1. SEM images of the as-received refractories surfaces.

fraction of pores than AM2 according with the SEM observation; the highest difference was in the amount of close pores (π_c was 52% higher in AM1). This difference could be associated to the presence of tabular alumina in AM1, characterized by the presence of close pores, and the incidence of graphite on close porosity [13]. The differences in the particle size distribution should also affect the porosity values of each refractory.

The DTA thermograms of both materials (Fig. 2) were very similar in the position and the intensity of peaks. The maximum temperature of the exothermic peaks identified by DTA in which weight loss (Δm) was also registered in the thermogravimetric analysis (Fig. 3) is reported in Table 1. The weight losses in the temperature range 300–600 °C were attributed to the organic resin transformations. They consist in condensation, oxidation, dehydration and decomposition reactions occurring simultaneously [14,15]. Up to 900 °C, H₂O generated by several reactions evolves, being the maximum evolution between 200 and 500 °C. At temperatures higher than 400 °C, CH₄, CO, H₂, a little amount of CO₂, benzene and phenol derivatives and aromatic polycyclic compounds are evolved [14,16]. Product of these reactions is a carbonaceous non grafitizable structure (glassy-carbon) susceptible to further oxidation. This structure has a partial ordering and tends to higher organization and defect annealing at temperatures above 1000 °C [14].

The weight losses displayed over 800 °C for AM1 and AM2 were assigned to the graphite oxidation [17]. Based on the facts that the refractories were fabricated by the same manufacturer and DTA peaks assigned to the resin transformation were located at the same temperatures for both materials, it may be

assumed that the resin and the crosslinking degree are basically the same for both bricks (despising the influence of the other components of the refractories that affect the curing process [14]). Therefore, considering TGA results, the amounts of organic binder and graphite would be higher in AM2. However, the graphite content determined by XRD was lower for AM2; this difference was attributed to the Rietveld method error (± 5 wt.%) together with the incidence of the flakes orientation on the intensity of the diffraction peaks. Additionally, the reactions of the antioxidant during the heating (at a relatively high rate) in the TGA run could lead to an incomplete oxidation of graphite. These factors also explained the difference in the weight percentages of graphite estimated by XRD and TGA in both refractory materials.

The DTA thermograms also exhibited an endothermic peak around 660 °C (at 676 °C for AM1 and at 670 °C for AM2), that corresponds to the melting point of aluminium added as antioxidant. At temperatures over 1000 °C, peaks with low definition were attributed to the spinel formation from solid state reaction between alumina and magnesia and/or to the antioxidant reactions. These reaction forms as products:

- (a) Al₄C₃ at $T < 1000$ °C by reaction of liquid Al with the more reactive C coming from the organic binder, or with graphite [18–21],
- (b) Al₂O₃ at $T > 1100$ °C by reaction of Al₄C₃ with CO coming from the graphite oxidation [19],
- (c) MgO-Al₂O₃ by direct reaction of liquid Al with MgO (s) or Mg (g) produced by carbothermal reduction of magnesia [18–21],

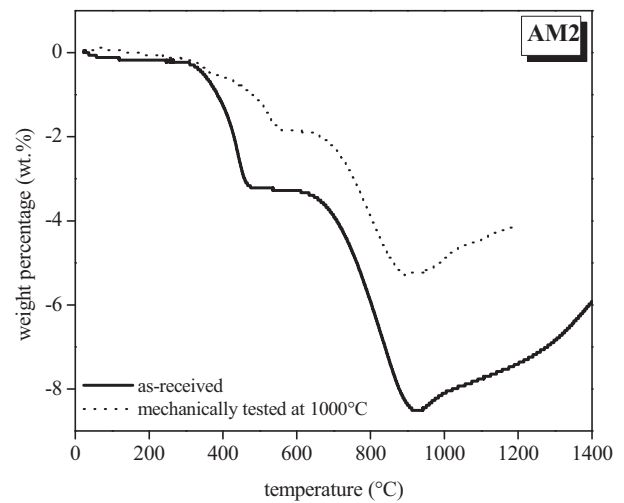
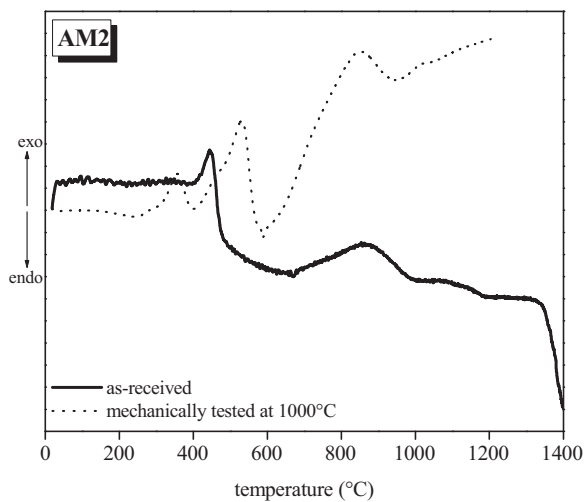
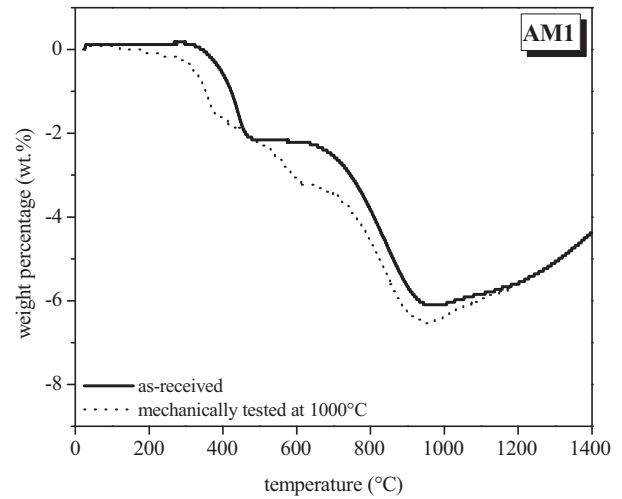
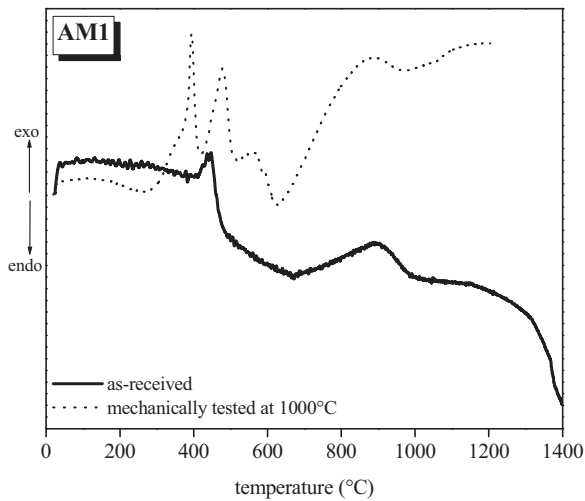


Fig. 2. DTA thermograms of as-received refractories and mechanically tested specimens (1000 °C).

Fig. 3. TGA thermograms of as-received refractories and mechanically tested specimens (1000 °C).

(d) SiO_2 at $T \sim 1100$ °C by reaction of silicon with the O_2 of the air; then, SiO_2 transforms to SiC by reaction with C [19].

The thermal expansion under load (0.6 MPa, Fig. 4) is in agreement with DTA/TGA data. Several changes in the slope of the AM1 curve were observed at temperatures below 700 °C. They were associated to the structural transformations of the resin described above plus the oxidation of the glassy-carbon product that generally involve a volumetric shrinkage [14,22] (decrease of the expansion rate). The alteration of the curve slope around 800 °C was associated with the graphite oxidation. It is worth mentioning that a volumetric shrinkage was registered near 1000 °C that might be associated to sintering assisted by load (the spinel formation, if occurs, is expansive). An estimation of the linear thermal expansion coefficient (α) ranged from $\sim 9.6 \times 10^{-6} \text{ }^\circ\text{C}^{-1}$ to $4.2 \times 10^{-6} \text{ }^\circ\text{C}^{-1}$. The first value was in agreement with α of the main components of the refractory (between $13.5 \times 10^{-6} \text{ }^\circ\text{C}^{-1}$ for MgO and $5.3 \times 10^{-6} \text{ }^\circ\text{C}^{-1}$ for mullite; a estimated “mean” value for graphite, considering the extreme

α values due of its high thermal anisotropy, is $13 \times 10^{-6} \text{ }^\circ\text{C}^{-1}$ [23] but its contribution to the thermal expansion of the composite refractory is almost negligible [23]) but higher than the values reported for this carbon-based material [14,24] due to

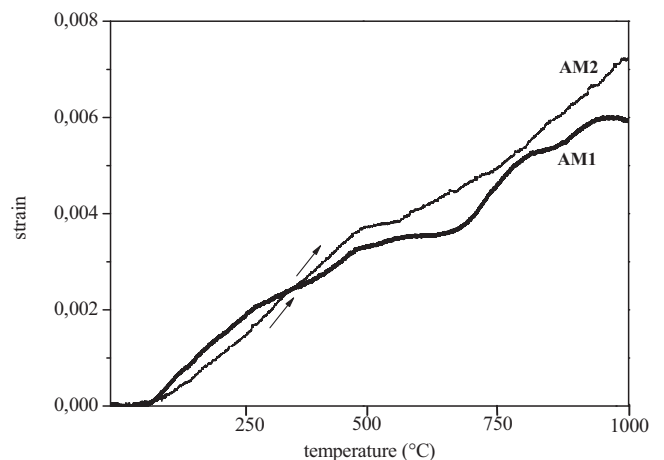


Fig. 4. Thermal expansion under load (0.6 MPa) curves.

the applied load. The reduction in α was attributed to the lower thermal dilation exhibited by the product of the resin transformation, mainly produced by the elastic restriction imposed by the crosslinked carbon network [14].

The expansion behavior of AM2 was similar to that of AM1, although the changes were less evident and even some of them were absent. The thermal expansion coefficients were in the range of the values estimated for AM1 but more homogeneous. These differences were attributed to the fact that the processes were not so well developed in AM2 refractory. Conversely to AM1, the curve of AM2 did not exhibit contraction near 1000 °C.

The differences between the expansion curves of both materials showed that the refractory AM1 suffered a higher degree of structural changes in respect to AM2 during the heating up to 1000 °C. Since it was considered that the cured resin was similar between both materials, being in a higher amount in AM2, it is possible that other factors influenced on the rate/extension of the transformation. On one hand, the higher apparent porosity in AM1 may favour the incoming of the surrounding gas. Even when the N₂ gaseous stream used in the mechanical test reduces the content of oxygen (by displacement and dilution) a little amount of this gas remains and it could encourage the processes [16]. On the other hand, the presence of other components of the refractory, in different proportion, type or granulometry, could alter the curing (generating a different crosslinking degree) as well as the pyrolysis of resin [14].

3.2. Mechanical tests

Stress–strain curves of AMC refractories at RT and 1000 °C are shown in Fig. 5 and the mechanical parameters are reported in Table 2. The elastic modulus and the mechanical strength of AM1 were higher than the values of AM2; the magnitudes were in general in the order of those reported in the literature for refractories of similar composition [20,24–26]. Overall, the stiffness and the mechanical strength were higher as the testing temperature increased. However, significant differences in the mechanical parameters with temperature were determined in AM2 whereas the values were not so dissimilar in AM1, especially the Young's modulus. In agreement with this fact, the strain to fracture showed only a little change with the testing temperature in AM1, but a significant reduction in AM2. The increment of the yield stress to σ_R ratio from RT to 1000 °C indicated a higher brittleness in the last condition.

Stress–strain curves at RT exhibited a marked deviation from linearity and a softening behavior, i.e., the gradual loss of the load bearing capacity and the stiffness during the mechanical loading (Fig. 5). In the case of AM1, only a little portion of the curve was

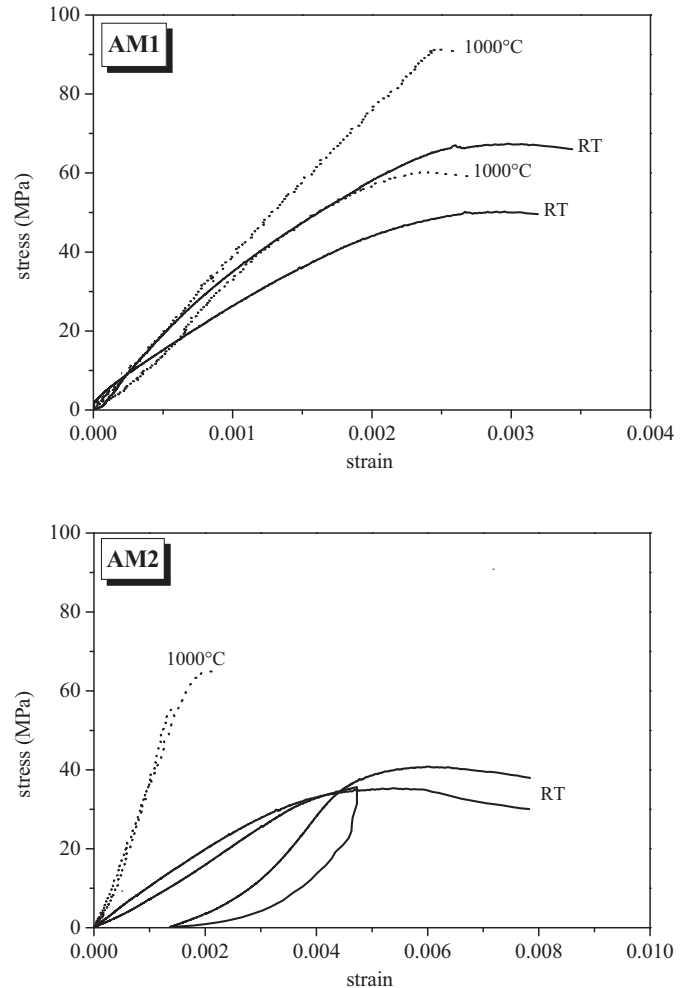


Fig. 5. Stress–strain curves at RT and 1000 °C.

linear, moving away from linearity rather early and showing a marked softening behavior as was manifested by the low σ_Y/σ_R . The non-linear response was less marked at room temperature in material AM2, even when the strain to fracture remained rather higher than the value of AM1. The occurrence of irreversible or residual strain, characteristic of those refractories containing graphite [26,27] was evident in the loading–unloading cycle in RT curve of AM2 (performed to re-locate the extensometer that reached the limit of the measure range before the end of the test).

In every case, the fracture run diagonally across the cylinder, as is characteristic of the compression tests where friction effects act in the contact area between the flat surfaces of the specimens and of the push-rods (or the disk between them). The cracks propagated mainly through the bonding phase surrounding the aggregates in several cases. The failure of the specimens had a higher ductile character at RT whereas at 1000 °C the fracture was quasi-brittle to brittle, in agreement with the increment in the σ_Y/σ_R ratio.

3.3. Post-testing characterization

The results of the characterization of the materials after the tests at high temperature are reported in Table 3.

Table 2
Mechanical parameters.

| | T (°C) | E (GPa) | σ_R (MPa) | ε_R (%) | σ_Y/σ_R (%) |
|-----|--------|---------|------------------|---------------------|-------------------------|
| AM1 | 20 | 32 ± 14 | 58 ± 12 | 0.30 ± 0.01 | 31 ± 9 |
| | 1000 | 37 ± 1 | 76 ± 21 | 0.24 ± 0.01 | 60 ± 7 |
| AM2 | 20 | 12 ± 5 | 38 ± 3 | 0.60 ± 0.05 | 70 ± 9 |
| | 1000 | 29 ± 8 | 60 ± 7 | 0.17 ± 0.06 | 85 ± 7 |

Table 3
Characterization of post-testing refractory materials.

| | | AM1 | | AM2 | | |
|-----------------------------------|--------------------------------|-------------|-----------|--------------------------------|-------------|-----------|
| Composition (XRD) | | | | Al ₂ O ₃ | | |
| | | | | MgO | | |
| | | | | C | | |
| ρ_{pic} (kg/m ³) | | 3580 ± 50 | | | | 3720 ± 50 |
| ρ_b (kg/m ³) | | 3000 ± 20 | | | | 3100 ± 20 |
| π_a (%) | | 11 ± 2 | | | | 8 ± 2 |
| π_r (%) | | 17 ± 2 | | | | 16 ± 2 |
| π_c (%) | | 5 ± 2 | | | | 8 ± 2 |
| DTA | 345 °C | 476 °C | 895 °C | 358 °C | 520 °C | 850 °C |
| Δm (TGA) | −1.6 wt.% | −1.6 wt.% | −3.7 wt.% | −0.6 wt.% | 1.2 wt.% | −3.4 wt.% |
| D_{50} (mm) | global | 1.35 ± 0.02 | | | 0.99 ± 0.02 | |
| | Al ₂ O ₃ | 1.58 ± 0.02 | | | 1.51 ± 0.02 | |
| | MgO | 0.79 ± 0.02 | | | 0.57 ± 0.02 | |

The same phases present in the original materials were identified in both refractories AM1 and AM2 after the tests at 1000 °C. No new peaks corresponding to phases coming from reactions of aluminium (Al₄C₃ or AlN) or to spinel were detected. This fact shows that if chemical changes occurred during the thermal treatment as can be inferred from DTA data of as-received materials, these reactions were not massive but occurred at a very local level (likely in the matrix) so that the product amount could be lower to the detection limit of the XRD technique. In fact, the overlapping of the diffraction peaks of spinel with others of the main phases could difficult its identification. Even when the detection of spinel has been reported in the literature already at 1000 °C [21,28], it has been generated from Al or by reaction of MgO with reactive alumina. Migliani and Uchno [4] was not detected spinel at 982 °C and Williams and Hagni [3] estimated a temperature around 1050 °C for the appearance of spinel in neutral atmosphere (not specified). This temperature is slightly higher than that used in the mechanical tests of the studied AMC refractories.

The DTA of high temperature tested specimens (Fig. 2) exhibited differences with those of the as-received materials mainly in the region of peaks corresponding to the resin transformation. Similar changes were observed in both refractories. The peak assigned to the pyrolysis of the organic binder in the original materials (440 °C) was not detected in none of the tested refractories, but other peaks were displayed in the low temperature region (<700 °C, Table 3) indicating an incomplete transformation and/or a higher susceptibility of the products to be oxidized. The resin decomposes by a complex mechanism briefly described above including several transformations and a wide range of temperatures. In those conditions suitable to assure a complete transformation and a high coke yield (50–60 wt.%), the gases evolution extends up to temperatures near 1000 °C and even at higher temperatures the ordering of the glassy-like carbon and the defect annealing continue [14]. The transformation of the resin could not be complete during the mechanical test due to several reasons: (a) the heating rate could be not slow enough to complete the processes (b) the existence of a thermal gradient into the specimens, mainly during the heating, due its limited thermal

conductivity and (c) the closeness between the testing temperature and that where the transformation stops.

Conversely, the peak assigned to graphite was located almost at the same position in tested and as-received materials but the weight loss was lower in the former (Tables 1 and 3). This fact was according with the superficial discoloring exhibited by the specimens after tests. The proportion of graphite oxidized during the mechanical test was superior in AM2 (~36%, twice the value of AM1).

Regarding aggregates sizes, a significant increment of the global size was observed in AM1 and AM2 after the mechanical tests at 1000 °C (between 20 and 30%). Alumina particles tended to be larger whereas periclase ones exhibited the opposite tendency; the changes were more pronounced in AM2. These facts showed that the transformations occurring in the materials due to thermal effects not only involved the binder but also the aggregates. Between the reactions explaining the granulometric variations registered are: the carbothermal reduction of MgO and the spinel formation. The carbothermal reaction $MgO(s) + C(s) \rightarrow Mg(g) + 1/2CO_2(g)$ and the further re-oxidation of Mg(g) with the little amount of oxygen in the N₂ stream used in the mechanical test could cause the growth of the alumina aggregates and the reduction in the size of magnesia ones. The MgO would recrystallize indistinctly on the surface of alumina or periclase aggregates. However, alumina particles were in higher proportions in both AMC refractories. Even when the literature reports higher temperatures to initiate carbothermal reduction, the occurrence of this reaction at temperatures lower than 1000 °C has been inferred in MgO–C refractories (unpublished data).

The spinel formation is often produced around the alumina aggregates [3,29] by its reaction with MgO in solid state or with Mg(g) formed by carbothermal reduction in gaseous phase [19–21,28]. Both reactions explain the size variation of alumina and magnesia aggregates. Moreover, the finer particles in AM2 could account for the higher extent of the modifications observed in this material, since the reduction of the magnesia particles size benefits the spinel formation [30]. Similarly, the higher specific surface of this material would favour the carbothermal reduction. Alumina particles of AM1 and AM2

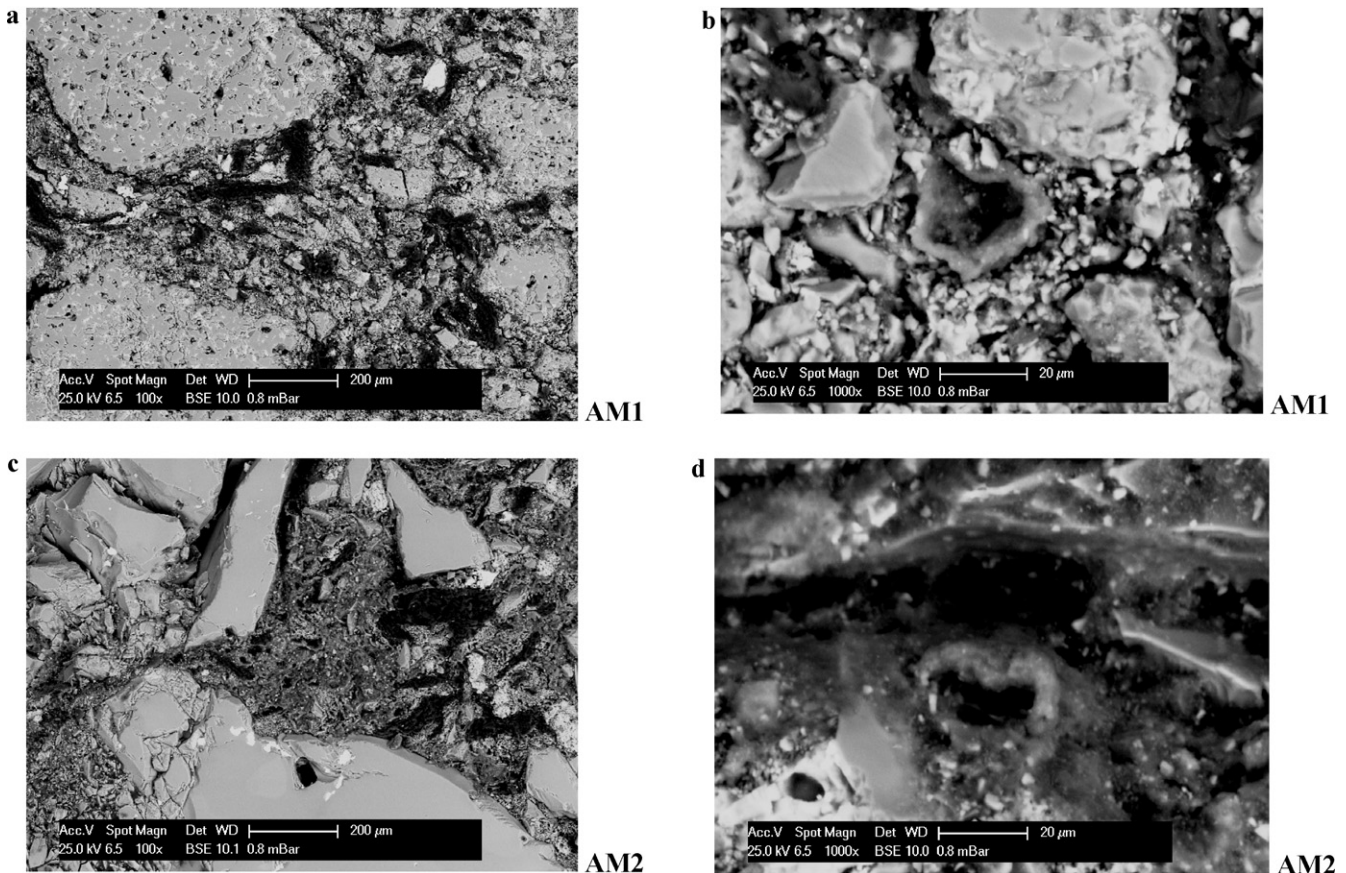


Fig. 6. SEM images of tested refractories surfaces (1000 °C).

specimens tested at 1000 °C and analyzed by SEM showed a peripheral rim having a different texture to those of the particle centre and of the bonding phase. In the EDS analysis of the rim, Mg was detected which can be as MgO or spinel. Anyway, these results demonstrated the occurrence of chemical reactions involving the aggregates of both refractories, more developed in AM2.

No evidence of massive formation of new phases during the test at 1000 °C were observed in the SEM/EDS analysis neither in AM1 nor in AM2, according with XRD data. SEM images of both refractories' surfaces are shown in Fig. 6. The aspect of the bonding phase was similar to that of the as-received material and particles of metallic additives without reaction were also observed [31]. Nevertheless, zones with different characteristics to those of the as-received materials were identified in AM1 and AM2 (Fig. 6b and d); the EDS analysis did not clarify their chemical composition. Similar microstructural features were reported in the literature and assigned to spinel coming from reaction of Al at 1600 °C [21]. In AM1 and AM2, those zones could be a product of an intermediate step in the spinel formation, Al_4C_3 or AlN, formed around 1000 °C and further dehydrated at room temperature [32]. In addition, the interface between some aggregates and the matrix exhibited a certain degree of decohesion and some damaged aggregates were observed (Fig. 6a and c).

After the high temperature test, the pycnometric density of AM2 was unchanged with respect to the original value where as

a decrease in ρ_{pic} was observed in AM1. Except the spinel formation, the rest of the reactions occurring up to 1000 °C (resin pyrolysis, lost of graphite by oxidation or carbothermal reaction, formation of Al_4C_3 or AlN) leads to a decrease of the solid density. The expansive character of the spinelization would also favour the higher thermal expansion registered in AM2 at the end of the heating (Fig. 4). Even when the spinel could not be identified by XRD or SEM/EDS, there are other signs indicative of a possible spinelization, more pronounced in AM2. Moreover, the difference in the solid density of Al_2O_3 (the component with the highest density that is replaced by spinel) and spinel is less than the half of the difference between the density of graphite and the rest of inorganic components. Then, in the case of AM2 the dominant effect was the graphite loss (higher than in AM1) opposing the possible effect of the spinelization, while in AM1 occurred the opposite.

The porosity parameters were modified after the high temperature test with the exception of the true porosity in AM1 that remained unchanged. In both refractories, the apparent porosity increased as was reported in the literature for this sort of materials [6,17,28] due to the volatiles elimination, the cracks generation by volumetric differential shrinkages and the graphite loss. The larger variation of π_a in AM1 was associated to the higher extension of the resin transformation in this material.

On the other hand, the value of π_c increased in AM2 and showed the opposite tendency in AM1. Among the changes

occurring in the resin is the closing of open micropores (produced by the crosslinking), being the maximum rate of this process between 800 and 1000 °C [14]; this process accounts for the behavior of AM2. The opposite trend in AM1 was attributed to the effect of densification by sintering (manifest in the thermal expansion curve) between particles in the matrix and also into the aggregates (taking into account the impurities level and the presence of glassy phase).

In AM1, the opposite effects of the close and the open porosities with the temperature up 1000 °C were equivalent, producing no change in the value of π_v . In the case of AM2, the true porosity increased mainly because of the close porosity increment. The spinelization is usually accompanied by generation of micropores [20] and cracks (during the cooling down) [30]. Therefore, if this process occurred in a local level at least, it contributed increasing the true porosity (mainly in AM2).

In summary, there are evidences of incomplete transformations after the mechanical testing at 1000 °C involving the carbonaceous binder (more developed in AM1), the graphite and also the aggregates. The latter includes the spinel formation as a possible process occurring in a higher extent in AM2. The reaction of metallic additives could not be confirmed. Moreover, in AM1 was inferred a certain degree of densification by sintering, without alteration of true porosity, whereas an increment in the true porosity was registered in AM2 according to the modification in the organic binder and the absent of sintering evidences.

4. Discussion

Bearing in mind the characteristics of the fracture of the mechanically tested specimens (cracks propagating through the matrix itself and also breaking the interface with aggregates) it is evident that the bonding phase has a fundamental role in the mechanical response. The modifications involving the aggregates at high temperature, indicates that they could be also involved in the mechanical response too as was observed in the SEM analysis (Fig. 6).

The fact that the matrix is the weakest link in the refractory structure and the main responsible on the mechanical behavior in cold and hot conditions is common in this sort of materials. In oxide-C refractories, the bonding phase is highly heterogeneous (novolaka or resol resin, binder, graphite flakes and fine particles of magnesia, alumina and antioxidants) with components having poorer mechanical properties than the aggregates and dissimilarities that create low surfaces affinities and discontinuities. These features lead to low cohesion and finally, to cracks. The quality of the matrix-aggregate interface is influenced by the fabrication methods and the particle characteristics (magnesia or alumina, sintered or electrofused, sources) among other things; this region is a weak point in the structure. However, these discontinuities are also an advantage for the thermal shock resistance of the refractory body. In addition, the matrix suffers chemical, microstructural and textural changes with temperature and atmosphere.

The quasi-brittle behavior of both refractories at RT related to the softening behavior is associated to the presence of graphite and mechanisms of irreversible deformation. They include [13,15,26,27]: (a) microcracking of pre-existent fissures in the matrix and between the matrix and the aggregates; (b) sliding and crumpling of graphite flakes; (c) plastic deformation of the flakes themselves by shear of the basal planes [14] or microplasticity of the binder [27]. The more marked softening in AM1, with a lower content of graphite, is attributed to the effect of its high true porosity (pores and cracks) favoring the microcracking.

At 1000 °C, the increment of the ratio σ_Y/σ_R in AM1 and AM2 indicates a higher brittleness, also observed in the fracture features. This behavior is mainly due to the loss of graphite leading to a decrease of the system flexibility. Furthermore, the resin and the produced glassy-carbon have high stiffness; the latter exhibits a brittle or quasi-brittle behavior up to ≈ 1100 °C [14,15]. Other modifications of the bonding phase that will be analyzed in the following, also contribute to this behavior. However, the mechanical behavior of both materials is not completely brittle and therefore similar mechanisms to those occurring at RT are also operative, considering that at 1000 °C the viscoplastic process are not active yet, in a massive way at least.

At RT, the Young's modulus of AM1 is rather high in comparison with the values for other carbon-based refractories [15,20,27]; AM2 has a significant lower elastic modulus. The strain to fracture of AM1 is only the half of the value of AM2, in accordance to its high stiffness. The differences in the quality (impurity contents including glassy phase and porosity) and the grain sizes of alumina aggregates between AM1 and AM2 are difficult to quantify. Even when AM1 has calcined bauxite (low purity and high porosity), it also contents a proportion of tabular alumina of high quality (high purity and low porosity). On the other hand, AM2 has aggregates of intermediate quality. Nevertheless, bearing the global differences between both materials in mind, it is considered that the high E value of AM1 is due to the presence of coarser high stiffness alumina grains including tabular alumina. On the other hand, the low Young's modulus of AM2 is mainly attributed to the higher content of graphite. Furthermore, the higher amount of resin and graphite in this refractory could promote the presence of a higher amount of cracks or larger sized cracks contributing to decrease the value of E .

The values of mechanical strength at RT are also different between AM1 and AM2. The same factors accounting for the difference in Young's modulus also explain σ_R values: graphite and resin contents (the components with lower mechanical strengths), characteristics of the more resistant particles (alumina), amount or size of critical defects limiting the fracture strength (as cracks).

The mechanical properties of both refractories enhance significantly at 1000 °C with the exception of the Young's modulus and strain to fracture of AM1, mainly due to the structural and compositional changes occurring in the carbonaceous component of the bonding phase. However, it is important to remember that the fracture features manifest the

relevance of the matrix and the matrix/aggregates interface in the mechanical behavior of these refractories.

In accordance with the post-characterization data, several processes contribute to the increment of E to more than twice the value at RT in the case of AM2:

- (a) the resin transformation, even incomplete, in a structure with high stiffness due to the elastic restriction imposed by the carbon network, and an equivalent mechanical resistance [14,22],
- (b) the reduction in the graphite content and, consequently, in the structure flexibility.
- (c) the formation, although incipient, of new phases from the metallic additive reactions as Al_4C_3 (or AlN) that has a high modulus [20] and a binding effect [31],
- (d) the recrystallization of magnesia coming from the carbothermal reduction with C; when it deposits on the surface of aggregates or into the open pores favors the overall cohesion by interparticles linking,
- (e) the cracks closure by the effect the mechanical loading, the temperature and/or the occurrence of expansive reactions.

These factors overcome the effect of the true porosity increment tending to a stiffness reduction and they also account for the increment in the mechanical strength. In agreement with the variation in these mechanical properties, the strain to fracture shows a remarkable reduction. Furthermore, if spinelization occurs even incipiently, it also favors the ceramic bond although the spinel is considered a low modulus phase in the case its formation is accompanied by microporosity [20].

The differences between AM1 and AM2 in relation to the above mentioned factors are: a higher extension of the resin transformation, a smaller reduction in the graphite content, a lower degree in the process modifying the aggregates' size (carbothermal reduction or spinel formation) and the occurrence of sintering. Even considering these differences, the same factors determining the increment of σ_R in AM2 are also applicable to AM1. The difference in the advance of each process is the reason for the smaller increment of the mechanical strength in the latter. The lower content of metallic antioxidant additives in AM1 could decrease the effectiveness of the binding effect at high temperature.

The behavior of the Young's modulus (and the strain to fracture) in AM1 is unexpected in this context, since the changes in the composition and microstructure should impact on the elasticity modulus, as happens in AM2. It is possible that the lower degree in the graphite loss is not compensated by the (low) degree of transformation contributing to increase the stiffness in AM1. In addition, it have to bear in mind the negative effects of the spinelization and the lower binding effect related to the smaller proportion of antioxidant in this refractory. Furthermore, the resin pyrolysis is not necessarily accompanied by a variation of stiffness, because it depends on the initial crosslinking degree and the organization level achieved by the glassy-carbon.

In summary, the mechanical behavior of commercial AMC refractories, both resin-based materials, shows marked differ-

ences at room temperature and at near the pre-heating ladle temperature (1000 °C). This fact indicates that their differences in composition and microstructure, both in a relatively narrow range, have a strong impact on mechanical properties and their changes with temperature. In fact, it is verified that this occurs even when the microstructural evolution of the refractories are very similar, having only differences in the extent of the processes. As a second stage of this work, the mechanical evaluation at operation temperatures (around 1600 °C) is planned for the future.

5. Conclusions

As a first stage in the obtainment and analysis of data about the mechanical behavior of commercial AMC refractories used in steelmaking ladles, stress–strain curves of two different resin bonded bricks AM1 and AM2 were determined at room temperature and at temperatures near the ladle pre-heating condition (1000 °C). A detailed analysis of the mechanical behavior based on a comprehensive material characterization, the using of conventional (mechanical strength and elastic modulus) and non-conventional mechanical parameters (yield stress and fracture strain) and a complete post-testing characterization data was carried out, which lead to the following conclusions:

- during the heating up to 1000 °C (in nitrogen) the transformation of resin was incomplete and the aggregates were also involved in the chemical changes; AM1 suffered a higher degree of structural changes related to resin transformation but the chemical reactions (including an incipient spinelization) advanced in a higher extent in AM2; different changes in the solid density and porosity occurred in each material mainly due to different contributions of resin pyrolysis, graphite oxidation, incipient spinelization and sintering.
- at RT, AM1 exhibited higher values of mechanical strength and Young's modulus, mainly attributed to the presence of coarser aggregates including tabular alumina; the more marked softening behavior displayed by AM1, even when the strain to fracture remained smaller than the value of AM2, was associated to the higher true porosity causing microcracking.
- from RT to 1000 °C, the fracture was more brittle (higher σ_Y/σ_R ratio) and the mechanical properties showed a significant enhancement, except the Young's modulus and the fracture strain of AM1; the structural and chemical changes occurring up to 1000 °C in AM1 and AM2 explained these variations.
- the unexpected behavior of the Young's modulus and the fracture strain of AM1 were attributed mainly to the small transformation degree of resin, graphite and aluminium.

Beside these achievements, this work reasserts that the characterization and evaluation of commercial refractory materials with the aim to give fundamentals to the experimental data is a very complex and challenge task, hardly to be performed in a conclusive way. Even then, valuable information to understand and enhance the refractory performance in

service and to give guidelines for the material design is obtained.

References

- [1] Y. Sasajima, T. Yoshida, S. Hayama, Effect of composition and magnesia particle size in alumina–magnesia–carbon refractories, in: Proceedings of the UNITECR'89, 1989, pp. 586–603.
- [2] M. Rigaud, P. Bombard, X. Li, B. Guérout, Phase evolution in various carbon-bonded basic refractories, in: Proceedings of the UNITECR'93, 1993, pp. 360–371.
- [3] P. Williams, A. Hagni, Mineralogical studies of alumina magnesia carbon steel ladle refractories, in: Proceedings of the UNITECR'97, 1997, pp. 183–192.
- [4] S. Miglani, J.J. Uchno, Resin bonded alumina–magnesia–carbon brick for ladles, in: Proceeding UNITECR'97, 1997, 193–201.
- [5] A.D. Gupta, K. Vickram, Development of resin-bonded alumina–magnesia–carbon bricks for steel ladle applications, *Interceram* 48 (1999) 307–310.
- [6] R.K. Koley, A.V. Rao, S. Askar, S.K. Srivastava, Development and application of Al_2O_3 – MgO – C refractory for secondary refining ladle, in: Proceeding of the UNITECR'01, 2001.
- [7] M. Kamiide, S. Yamamoto, K. Yamamoto, K. Ankara, N. Kido, Damage of Al_2O_3 – MgO – C brick for ladle furnace, *J. Tech. Assoc. Refract. Jpn.* 21 (2001) 252–257.
- [8] A.A. Nourbakhsh, Sh. Salarian, S.M. Hejazi, S. Shojaei, F. Golestani-Fard, Increasing durability of ladle lining refractories by utilizing Al_2O_3 – MgO – C bricks, in: Proceeding of the UNITECR'03, 2003, 499–502.
- [9] A. Shojai, H. Sarpoolaky, F. Golestani-Fard, The effect of particle size distribution and magnesia amount and particle size on characteristics and properties of AMC refractories, in: Proceeding of the UNITECR'05, 2005.
- [10] C. Schacht, Needed fundamental thermomechanical material properties for thermomechanical finite element analysis of refractory structures, in: J. Bennett, J.D. Smith (Eds.), *Fundamentals of Refractory Technology*, Ceramic Transactions vol. 125, The American Ceramic Society, Westerville, 2001, pp. 93–101.
- [11] DIN EN 993-1, Method of Test for Dense Shaped Refractory Products. Determination of Bulk Density, Apparent Porosity and True Porosity (DIN 51056), 1995.
- [12] ASTM 329-88, Standard Test Method for Specific Gravity of Fired Ceramic Whiteware Materials, 1994.
- [13] M. Hampel, C.G. Aneziris, Evolution of microstructure and properties of magnesio–carbon refractories during carbonization: effect of grain size and graphite, *cfi/Ber DKG* 84 (2007) 125–131.
- [14] B. Rand, B. McEnaney, Carbon binders from polymeric resins and pitch Part I – pyrolysis behaviour and structure of the carbons, *Brit. Ceram. Trans. J.* 84 (1985) 165–175.
- [15] A.M. Fitchett, B. Wilshire, Mechanical properties of carbon-bearing magnesia-III. Resin-bonded magnesia and magnesia-graphite, *Brit. Ceram. Trans. J.* 83 (1984) 73–76.
- [16] A. Gardziella, Suren, M. Belsue, Carbon form phenolic resins: carbon yield and volatile components—recent studies, *Interceram* 41 (1992) 461–467.
- [17] W. Vieira, B. Rand, Microstructure development in pitch-containing alumina–carbon refractory composites, in: Proceedings of the UNITECR'97, 1997, pp. 851–859.
- [18] A. Yamaguchi, Application of thermochemistry to refractories, in: J. Bennett, J.D. Smith (Eds.), *Fundamentals of Refractory Technology*, Ceramic Transactions vol. 125, The American Ceramic Society, 2001, pp. 157–170.
- [19] C. Taffin, J. Poirier, The behaviour of metal additives in MgO – C and Al_2O_3 – C refractories, *Interceram* 43 (1984) 354–358 [5]/458–460 [6].
- [20] C. Baudin, High temperature mechanical behaviour of magnesia graphite refractories, in: J. Bennett, J.D. Smith (Eds.), *Fundamentals of Refractory Technology*, Ceramic Transactions vol. 125, The American Ceramic Society, Westerville, 2001, pp. 73–92.
- [21] M. Bavand-Vandchali, F. Golestani-Fard, H. Sarpoolaky, H.R. Rezai, C.G. Aneziris, The influence of *in situ* spinel formation on microstructure and phase evolution of MgO – C refractories, *J. Eur. Ceram. Soc.* 28 (2008) 563–569.
- [22] G. Bhatia, R.K. Aggrwal, M. Malik, O.P. Bahl, Conversion of phenol formaldehyde resin to glass-like carbon, *J. Mater. Sci.* 19 (1984) 1022–1028.
- [23] C.F. Cooper, The role of graphite in the thermal shock resistance of refractories, *Brit. Ceram. Trans. J.* 84 (1985) 57–62.
- [24] A. Watanabe, H. Takahashi, S. Takanaga, N. Goto, O. Matsuura, S. Yoshida, Thermal and mechanical properties of Al_2O_3 – MgO – C , *Taikabutsu Overseas* 10 (1990) 137–141.
- [25] B. McEnaney, B. Rand, Carbon binders from polymer resins and pitch. Part II – structure and properties of carbon, *Brit. Ceram. Trans. J.* 84 (1985) 193–198.
- [26] N. Schmitt, Y. Berthaud, J. Poirier, Tensile behavior of magnesia carbon refractories, *J. Eur. Ceram. Soc.* 20 (2000) 2239–2248.
- [27] J.M. Robin, Y. Berthaud, N. Schmitt, J. Poirier, D. Themines, Thermo-mechanical behaviour of magnesia–carbon refractories, *Brit. Ceram. Trans.* 97 (1998) 1–10.
- [28] M. Bavand-Vandchali, H. Sarpoolaky, F. Golestani, H.R. Reazie, Atmosphere and carbon effects on microstructure and phase analysis of *in situ* formation in MgO – C refractories matrix, *Ceram. Int.* 35 (2009) 861–868.
- [29] M. Kamiide, S. Yamamoto, K. Yamamoto, K. Nakahara, N. Kido, Damage of Al_2O_3 – MgO – C brick for ladle furnace, *J. Tech. Assoc. Refract. Jpn.* 21 (2001) 252–257.
- [30] M. Rigaud, S. Palco, N. Wang, Spinel formation in the MgO – Al_2O_3 system relevant to basic refractories, in: Proceeding of the UNITECR'95 – vol. 1, 1995, 387–394.
- [31] S. Uchida, K. Ichikawa, K. Niihara, High-temperature properties of unburned MgO – C bricks containing Al and Si powders, *J. Am. Ceram. Soc.* 81 (1998) 2910–2916.
- [32] A.S. Gokce, C. Gurcan, S. Ozgen, S. Aydin, The effect of antioxidant on the oxidation behavior of magnesia–carbon refractory bricks, *Ceram. Int.* 34 (2008) 323–330.